General Disclaimer

One or more of the Following Statements may affect this Document

- This document has been reproduced from the best copy furnished by the organizational source. It is being released in the interest of making available as much information as possible.

- This document may contain data, which exceeds the sheet parameters. It was furnished in this condition by the organizational source and is the best copy available.

- This document may contain tone-on-tone or color graphs, charts and/or pictures, which have been reproduced in black and white.

- This document is paginated as submitted by the original source.

- Portions of this document are not fully legible due to the historical nature of some of the material. However, it is the best reproduction available from the original submission.

NASA Technical Memorandum 78520

Experimental Investigation of Wing Fin Configurations for Alleviation of Vortex Wakes of Aircraft

Vernon J. Rossow

November 1978

National Aeronautics and
Space Administration

NASA Technical Memorandum 78520

Experimental Investigation of Wing Fin Configurations for Alleviation of Vortex Wakes of Aircraft

Vernon J. Rossow, Ames Research Center, Moffett Field, California

NASA
National Aeronautics and
Space Administration

Ames Research Center
Moffett Field, California 94035

NOMENCLATURE

AR	aspect ratio
b	wingspan
b'	spanwise separation between trailing vortices
C_D	drag coefficient, $\frac{\text{drag}}{[(1/2)\rho U_\infty{}^2 S]}$
C_{D_i}	induced drag coefficient
C_L	lift coefficient, $\frac{\text{lift}}{[(1/2)\rho U_\infty{}^2 S]}$
C_ℓ	local lift coefficient
C_l	rolling-moment coefficient, $\frac{\text{rolling moment}}{[(1/2)\rho U_\infty{}^2 Sb]}$
$C_{l_{f_o}}$	rolling-moment coefficient on following model when generating model has no fins
C_M	pitching-moment coefficient
C_μ	$\frac{\text{jet momentum}}{qS_{fin}}$
c	wing chord
$\bar{c}$	mean geometric chord
c_{fin}	chord of fin
h_{fin}	height of fin, $\frac{b_{fin}}{2}$
L	lift
$\ell(y)$	local spanwise lift
q	dynamic pressure, $\frac{1}{2}\rho U_\infty{}^2$
r	radius
Re	Reynolds number, $\frac{\rho U_\infty \bar{c}}{\mu}$
S	wing area
t	time

U_∞	free-stream velocity aligned with x-axis
u,v,w	velocity components in x-, y-, and z-directions
v_θ	circumferential velocity
x,y,z	coordinates; x, streamwise, y, spanwise, and z, vertical
y_{fin}	spanwise location of fin from aircraft centerline
α	angle of attack
Γ	circulation
γ	circulation in point vortices
μ	viscosity
ρ	air density

Subscripts

f	following model that encounters wake
fin	characteristic of fin mounted on wing
g	model that generates wake

EXPERIMENTAL INVESTIGATION OF WING FIN CONFIGURATIONS FOR ALLEVIATION OF VORTEX WAKES OF AIRCRAFT

Vernon J. Rossow

Ames Research Center

SUMMARY

A variety of fin configurations were tested on a model of the Boeing B747 in the 40- by 80-Foot Wind Tunnel at Ames Research Center and in the Ship Model Basin at Hydronautics, Inc., near Laurel, Maryland. The test results confirmed that a reduction in wake rolling moment is brought about by the vortex shed by the fins so that a wide range of designs can be used to achieve wake alleviation. It was also found that the reduction in wake-induced rolling moments is especially sensitive to the location of the smaller fins on the wing and that the penalties in lift and drag can probably be made negligible by proper fin design.

INTRODUCTION

Research directed at wake vortex minimization was undertaken by NASA because the persistent nature of the vortices that trail from the wings of subsonic transport aircraft create a hazard for following aircraft. This hazard is most evident near airports where aircraft are usually constrained to a specified flight corridor during landing operations. The present solution to the problem is to set the separation distances large enough (e.g., up to six miles) to allow time for the vortices to either decay or move out of the flight corridor so that safety is not compromised. Such a solution is unsatisfactory because it limits the runway utilization rate. The NASA wake vortex research program is therefore directed at finding aerodynamic means to increase the dispersion or dissipation rate of vortex wakes of aircraft so that separation distances can be safely decreased to about two miles. Furthermore, the modifications to be used for wake alleviation should not have significant detrimental effects on aircraft performance.

The NASA program (ref. 1) considered both the fundamental aspects of wake vortices and methods whereby the velocity and/or the rolling moments in the wake could be reduced. The alleviation mechanisms that were investigated fall into a group which injects turbulence (refs. 2-5) into the wake to dissipate the vortices or a group which uses vortex interactions (refs. 6-16) to disperse wake vorticity. Some ineffectual attempts to solve the problem were relegated to honorable mention in an article by Dunham (ref. 17).

The research directed at finding lifting configurations that produce favorable vortex interactions for wake alleviation led to the concept of vortex injection (ref. 16). That is, a vortex is injected into the wake of a

wing so that the modified wake disperses due to its self-induced velocity field. Although the vortex may be injected by a variety of devices, vertical surfaces or fins mounted on the wing and lifting sideways were used to modify the vortex wake of a model of the Boeing 747. The objectives of the tests reported in reference 16 were to optimize the fin configurations and to find the extent to which the wake could be alleviated. The design of the fin configurations were initially based on approximate theoretical guidelines and on numerical calculations of vortex wake dynamics with and without vortex injection. Although the effectiveness and theoretical basis of the concept were proven by the data presented in reference 16, it was felt that alternatives to rectangular fin shapes should be investigated to find out if the overall size could be reduced further without a substantial reduction in effectiveness. The tests in the wind tunnel and water tow tank described herein were therefore conducted to extend the investigation of rectangular fins reported in reference 16 by evaluating a variety of other fin shapes and sizes. These results increase the choices available to manufacturers for wake vortex alleviaton schemes.

RELATIONSHIP OF FIN SIZE TO WAKE ALLEVIATION

The test results obtained with wing fins of rectangular planform indicated that the alleviation in rolling moment was approximately proportional to the strength of the vortex shed by the fin (see fig. 9 of ref. 16). Furthermore, the height at which the vortex was injected did not appear to alter its effectiveness as long as the height was below about 0.15 b_g. These experimental results therefore indicate that comparable wake alleviation should be obtainable with any wing fin (or other device) that sheds a vortex of the same strength at the same spanwise location. Minimization of the fin size (i.e., wetted area) should then be related to the maximum lift or side force which the fin can produce. That is, since the strength of the fin vortex is to remain constant between fin configurations, the fin size, S_{fin}, and fin vortex strength, Γ_{fin}, are related to the lift on the fin by

$$\text{lift} \approx \frac{\rho U_\infty^2}{2} S_{fin} C_{L_{fin}} = -\rho U_\infty \Gamma_{fin} b'_{fin}$$

If the ratio of the strengths of the vortex shed by the fin to that shed by the wing is held constant, it is then found that

$$\frac{\text{fin lift}}{\text{wing lift}} = \frac{S_{fin} C_{L_{fin}}}{S_g C_{L_g}} = \frac{\Gamma_{fin} b'_{fin}}{\Gamma_g b'_g}$$

or, with

$$\frac{b'_{fin}}{b'_g} \approx \frac{b_{fin}}{b_g}$$

$$\frac{\Gamma_{fin}}{\Gamma_g} = \frac{C_{L_{fin}}}{C_{L_g}} \quad \frac{\bar{c}_{fin}}{\bar{c}_g}$$

Therefore, if the fin size (chord in this case) is to be reduced, the lift coefficient on the fin must be increased proportionately so that the product is constant.

For these reasons, a variety of fin shapes and sizes were considered in the investigation reported here. The objective was to find the smallest possible configurations that still retain the alleviation achieved with rectangular fins. Since rectangular fins of small aspect ratio have a maximum lift coefficient of approximately one, the fin designs being sought should have a maximum lift as much above one as possible.

FIN CONFIGURATIONS

The foregoing discussion points to the need for fins which develop large lift coefficients. Furthermore, it is the strength of the vortex rather than the shape of the fin that is the dominant parameter for alleviation. A search of the literature (e.g., refs. 18-30) suggested a variety of fin configurations which might develop lift coefficients in excess of one, permitting a reduction in fin size. The configurations chosen for study in this investigation are illustrated in figure 1. In addition to the configurations shown, several of the fins were tested in pairs. For example, two triangular fins or two circular arc fins (fig. 2(c)) were placed near each other near the 50% semispan location on the wing and at the same angle of attack to the free stream. The fins were not close enough to be considered a multi-element fin but they were usually about one fin chord apart — close enough that their effect on alleviation was complementary.

The $C_{L_{max}}$ values listed in figure 1 with the sketches of the various fin shapes were obtained at larger Reynolds numbers than those used in the present tests. Also, the values presented in figures 1(b), 1(d) and 1(f) are based on results for two-dimensional or large aspect ratio configurations. Therefore, when the fins are installed on an aircraft wherein the local flow direction and magnitude vary considerably over the wing upper surface, the performance and lift of the fin tested might be different than anticipated from the tests used in the references cited. Each fin shape was made in a range of sizes wherein the height was varied from 0.0142 b_g (i.e., 1 in./70.5 in.) to 0.071 b_g (5 in./70.5 in.) in 0.0071 b_g increments in order to cover the range of alleviation capability of the configuration. Of the fins that were made, only enough of each type were tested to determine the sizes required to adjust the rolling moment in the wake from $C_{l_f} \approx 0.04$ to 0.10.

The angle of attack relative to the free stream and the location of the fins on the wing were set by use of templates to insure repeatability. The angle of attack could therefore be changed easily and with repeatability from -36° to +36° in 6° increments. The fin angle of attack is considered positive

(fig. 2(b)) when the vortex shed by its tip is of the same sign as the one shed by the nearest wing tip. Since the number of possible test conditions is large and the availability of test time limited, the test locations and angles of attack were usually restricted to those found to be near optimum for rectangular fins.

TEST FACILITIES

Experiments were conducted in the 40- by 80-Foot Wind Tunnel at Ames Research Center (fig. 2) and in a water tow tank[1] (fig. 3) 125 m long by 7.6 m wide by 3.8 m deep, located at Hydronautics, Inc. Each facility has special features which permitted simulation of various aspects of the wake alleviation to be expected in a full-scale or flight experiment. The wind tunnel yields continuous wake data at downstream distances up to about 14 spans (e.g., fig. 2 and refs. 1, 12, and 16). During a typical run the following model is held fixed at various vertical and lateral positions in the wake for about one minute (see refs. 4 and 12 for more details on test procedures). The rolling moment at each position fluctuates due to motion or meander of the wake of the B747 model used as generator. The maximum value measured at each location is then used to map out rolling moment contours (e.g., fig. 4 here and fig. 5 of ref. 31) and to determine the maximum for that configuration. These tests were usually conducted at 13 to 14 spans downstream of the generator model.

In the water tow tank, data is obtained on an intermittent basis because the models are towed through the water over the finite length of the channel (125 m or 410 ft). The follower and generator carriages (fig. 3) move independently at the same speed (~3.8 m/s or 12.5 ft/s) separated by a predetermined time interval that establishes a 46-span separation distance. During each passage of the carriages along the tank, the following model is moved on a vertical path through the generator wake so that the rolling moment is surveyed along a given lateral segment of the wake. After four to six such passages at various lateral positions of the following model (with 15 to 20 min between runs to allow flow disturbances from the previous run to decay to less than about 1 mm/s), a maximum rolling moment for each configuration is determined. Even with such low residual velocities, the large downstream distances often permitted sufficient time for the vortices to move or meander enough that several nearly equal maximums[2] occurred during a single vertical traverse of the following model. Further details of the test set up and procedures are presented in references 1, 12, 16, 17 and 31.

---

[1]The tests in the Ship Model Basin at Hydronautics, Inc. (located near Laurel, Maryland) were carried out under NASA Contract NAS1-15189 which was arranged for and monitored by G. Thomas Holbrook and R. Earl Dunham, Jr. of Langley Research Center.

[2]The magnitude of the residual velocities were estimated from the distances observed for this meander of the vortex center during the time interval between passage of the two carriages.

In both tests being reported here, the B747 models used to generate the wake were mounted from the top of the fuselage to minimize interference of the strut wake with the lift-generated wake. The flaps were in full landing position (30°/30°), the landing gear were fully extended, and the horizontal tail was set at 0° relative to the fuselage or aircraft reference plane (i.e., the horizontal tail is at 0° when the aircraft is at 0°). In the wind tunnel, a few configurations were tested at α_g = 0°, 4°, 8°, and 12°. Most however, were tested only at 4° ($C_{L_g} \approx 1.2$) to expedite the investigation of a wider variety of configurations. In the water tow tank the model was set at α_g = 5° so that $C_{L_g} \approx 1.2$. A larger α_g was believed to be required in the water tow tank because the wing tips of the generator model were only 0.4 b_g below the free surface of the water. As a result, the water surface deflects considerably as the B747 model moves so that the span loading and wake structure probably differ from those obtained in the wind tunnel where wall effects are negligible. Differences in the test results from the two facilities may then be caused by the presence of free surface interference in the water tow tank not present in the wind tunnel. For example, measurements made with the (30°/0°)[3] B747 configuration (e.g., refs. 1 or 12) indicate that the nearness of the free surface probably causes the delay from 14 b_g in the wind tunnel to 45 b_g in the tow tank observed to take place in the favorable vortex interactions responsible for the alleviation achieved with that configuration. It is not certain whether the higher level of background turbulence in the wind tunnel has an influence on the test results.

The general characteristics of the models and of the test parameters used in the tests are tabulated in table I.

TEST RESULTS

The large number of fin configurations and test parameters made it impossible to thoroughly evaluate the various possibilities with the available wind tunnel time. A few of the more promising configurations were tested in more detail than the others, but most were tested at selected conditions to obtain a cursory evaluation of the alleviation effectiveness of the fin. These wind tunnel tests were used to screen the variety of fin shapes shown in figure 1 so that the most promising designs could be tested at the greater downstream distances available in the water tow tank. As a result, only the fins with circular arc planform (fig. 1(e)) were tested in the tow tank. In the discussion to follow, the data obtained in the two facilities will be compared with each other and with the rectangular fin data of reference 16 so that the graphs summarize most of the existing fin data. In these comparisons, it should be remembered that the wind tunnel data was taken at x_f/b_g = 14 and the water tow tank data at x_f/b_g = 46. Furthermore, a slightly larger angle

[3]This notation is used to designate the deflection of the inboard and outboard flaps, respectively. A 30° deflection puts a flap in the position used for landing.

of attack was needed in the tow tank ($\alpha_g = 5°$) to achieve $C_{L_g} = 1.2$ as compared with the wind tunnel ($\alpha_g = 4°$). To distinguish the data obtained in the two facilities, the wind tunnel data will be designated by open symbols and the tow tank data by solid symbols. Numerical values for the various aerodynamic parameters in the two facilities for the generator and follower models are presented in tables II and III.

Fins With Triangular Planform

Wake imposed rolling moments on the following wing were measured in the wind tunnel behind the B747 model equipped with various configurations of triangularly shaped fins. The variation of the maximum rolling moment found in the wake as a function of angle of attack and fin size and with one or two fins per side is compared in figures 5, 6, and 7 with results for rectangular fins from reference 16. It is noted that two triangular fins (indicated by a double line) are usually more effective than a single fin, but not necessarily superior to a single rectangular fin of less wetted area (e.g., fig. 5). Since the ratio of the height and chord of the triangular fins is held fixed by the semiapex angle of the fin, the area changes more rapidly than that of the rectangular fins because only the height changes. It is not surprising then that the curves in figure 7 appear to switch from approximating one rectangular fin curve to the other. A clear superiority of either the rectangular or triangular fin shape is not evident in the present data. This result is not surprising since triangularly shaped flat plates do not develop lift coefficients much greater than rectangularly shaped ones (i.e., both have a $C_{L_{max}} \approx 1$).

Fins With Circular-Arc Planform

As indicated previously, a set of circular arc fins was made with the Clark-Y section to duplicate the wings studied by Zimmerman (ref. 19) and another set with the GA(W)-2 section (ref. 21) to see if a more recent airfoil design would yield improved performance. Since preliminary results were promising, these two fin designs were tested more thoroughly in the wind tunnel than other designs and they were the only ones investigated in the water tow tank. Data from the two test facilities are compared in figures 8 to 13 with the data for rectangular fins presented in reference 16. Throughout the comparisons, the open symbols are used to denote measurements in the wind tunnel and the solid or filled symbols those in the water tow tank.

The circular arc fins were placed at larger angles of attack than any of the other fins because the data of Zimmerman (ref. 19) indicated that circular wings do not stall until they reach 45° angle of attack. Since the flow angularity over the generator wing is uncertain, the true angle of attack of the fin is unknown. Neither of the two fins made of semicircular shapes appears to provide a completely linear increase in alleviation at the higher angles of attack. This result may be caused by the boundary layer on the wing, the low Reynolds number of the flow over the fin, or other effects. Nevertheless, the alleviation is significant for both airfoil sections and the two are in good

agreement. When the Reynolds number is increased to flight values, the fins may retain their lift effectiveness more completely to higher angles of attack and thereby provide more alleviation.

The smaller fins were found to provide alleviation over a smaller spanwise location on the wing (fig. 9) than the larger rectangular fins. As a consequence more testing is required to be certain that the smaller fins are in their optimum location, since a location too far inboard causes a rolling moment larger than the conventional configuration. All of the fin configurations exhibited the same sensitivity to spanwise location as the chord of the fin was reduced.

The data in figures 10 and 11 show that fins with semicircular planform provide as much or more alleviation than rectangular fins of the same dimensions. Furthermore, two circular arc fins, located within about one fin chord of each other, are more effective than single fins and may be easier to install onto flight hardware than one larger fin. In both figures 10 and 11, the port and starboard sides of the wake are noted to yield different rolling moments. This difference consistently appeared in both facilities even though different B747 models were used. Although different models were used in the two facilities, the wind tunnel model was made of fiberglass by using the steel water tow tank model as a mold. It is not surprising then that both models exhibited similar asymmetries.

The lift and drag on the B747 model is shown in figure 12 for the rectangular and circular arc fins. The results indicate that properly designed fins can reduce the associated penalties and, in fact, can increase the lift and reduce the drag of the conventional B747 landing configuration. It is felt that the vortices shed by the fins enhance the velocity field over the wing so that flow separation is reduced and the overall flow improved. Penalties due to weight and installation costs of the fin still exist, but the results obtained with the smaller fins (and reduced alleviation) indicate that further optimization may lead to configurations wherein the wake rolling moments have been reduced to the desired level and the lift and drag penalties are negligible.

A direct numerical comparison of the data in table III for the tests of circular arc fins in the water tow tank can be made with the data in table II for the corresponding tests in the wind tunnel. Some of this data is also presented in figure 13 on an expanded scale so that a graphical comparison can be made of the data from the two facilities. In general, there is little change in the level of C_{l_f} over the range of x tested in the two facilities. Where substantial differences occur, it is believed that the optimum fin position in one facility was not the same as in the other. Also, the proximity of the B747 model to the free surface of the water in the tow tank and the likelihood of cavitation on the fins (especially at $\alpha_{fin} = 30°$) may have influenced the wake dynamics so that some configurations differ more than others. From an overall view, the two sets of data do not differ appreciably even though the downstream distance to the follower is over three times as large in the tow tank as in the wind tunnel and the tow tank model is only $0.4\ b_g$ from the free surface of the water.

Multielement Fins

Several fin configurations, which had several airfoil sections in close proximity (figs. 1(b) and 1(c)), were tested in the wind tunnel. Some of these results are listed in table II but not shown graphically because the alleviation achieved was inferior to simpler fin configurations. Although the section lift coefficients achievable with multielement airfoils is high, they may lose their advantage at low aspect ratios or when placed on a reflection plane like the generator wing which has a boundary layer. Further consideration of multielement fin configurations should first investigate the performance of the fin when isolated from a generator model. The relationship of alleviation to the number of and separation distance between airfoil elements also needs study because two fins placed one to two chord lengths apart near the optimum spanwise location yielded improved alleviation for all fin shapes tried. In those cases the spacing of the elements was probably not small enough to produce a strong multielement airfoil effect but close enough that the fins complemented one another. Other fin shapes were tried that had several elements in close proximity to generate strong interactions. Of those tried, only the two element fins made of bent plates (fig. 1(b)) were noticeably better than a single element.

Fins With Blown Flap

Since the optimum fin location is in the vicinity of the inboard engine on the B747 model, it seemed likely that excess high pressure air from the engine could be used to enhance the lift or side force capability of the fins by chordwise blowing (fig. 1(f)). At the end of the test period a single blown flap configuration was tested at one location on the wing. The results are presented in table II for the one fin at two angles of attack and for the maximum blowing available (C_μ was estimated at about 0.5) with the test set up. The fin at the larger angle of attack provided significant alleviation but there was no time to optimize the various fin parameters. These preliminary results indicate that further consideration should be given to the fin location (x_{fin} and y_{fin} on the generator wing) and to its angle of attack to see if greater alleviation can be achieved with fins having blown flaps. Also the use of two or more fins on each wing should be tried as a method for reducing the size or wetted area of the fins with blowing.

Comparison of Fin Configurations

The direct and nearly linear relationship found in reference 16 between alleviation (i.e., $(C_{l_{f_o}} - C_{l_f})/C_{l_{f_o}}$) and fin vortex strength led to the investigation described here. The details of the mechanism whereby the fin vortex alleviates the wake velocities appears to be complex and to involve vortex merger and redistribution of the lift-generated wake components. The data presented here does not clarify the alleviation process but it does describe a variety of fin configurations which yield reduced wake rolling moments. A comparison of the fin configurations that were tested can now be made to see if trends and optimums can be identified.

One means for comparison is to specify that the optimum fin is one that reduces the wake rolling moment a given amount and that also causes a mimimum penalty in lift, drag, weight, and so on. Such a graphical comparison is made in figure 14. The measured rolling moment for the devices investigated is shown as a function of the ratio of the wetted area of the fins to that of the wing. A data point as near as possible to the origin is desired so that both the wake induced rolling moment and the required fin size are small, (a small fin is presumed to impose a smaller penalty than a larger fin.) In this comparison, the angle of attack of the B747 model was held constant during the tests so that the lift was approximately $C_{L_g} = 1.2$ in both test facilities. The data falls in a band about the rectangular fin data. Of most interest are those that are lowest — the circular arc and the blown flap fin configurations. The data point in figure 14 for the fin with a blown flap does not, however, necessarily represent the lowest rolling moment achievable with that fin because the time needed to optimize its spanwise location, angle of attack, etc., was not available. Since the water tow tank facility was not set up to test blown flap configurations, those particular tests concentrated on the circular arc fins.

EFFECT OF RECTANGULAR FINS ON SPAN LOADING

The fins redistribute the loading on the wing as shown in figure 15. The span loadings were calculated using a vortex lattice method developed by Hough (ref. 32). It is noted in figure 15 that the larger rectangular fin changes the loading substantially over a portion of the span but the smaller rectangular fin makes only small local changes. The alleviation brought about by the two fin arrangements is noted in figure 11 to be about the same, suggesting that some characteristic other than span loading must be the dominant factor in producing the alleviation achieved by the fin. It is to be noted that the rolling moment contours (fig. 4) for the fin-modified wake are shaped quite similarly to those of the unmodified wakes (fig. 4(a) of this page and fig. 5 of ref. 31), but the magnitudes of the overturning moments are greatly reduced (fig. 4(b)). The fin appears to redistribute the wake vorticity so that the interior of the vortex has reduced velocities but the outer parts are hardly changed because the contours for $C_{l_f} = 0.01$ are about the same for both configurations in figure 4. That is, even though the contour for $C_{l_f} = 0.01$ is the same, the rolling moment for the conventional wake is over 0.12 at the center whereas the fin modified wake rises to only about 0.04 near its center. Such a large difference in rolling moments for a small change in span loading indicates that alleviation can be accomplished by balancing the wake vortex distribution so that favorable interactions occur.

WAKE STRUCTURE FOR VARIOUS ALLEVIATION SCHEMES

Figure 16 compares schematically the wakes of the conventional and the alleviated wakes studied to date in the NASA wake vortex program. It is

obvious that the number of vortices in the wake is not the determining factor for alleviation because the (30°/0°) configuration (gear up) wake with six wake vortices imposed rolling moments much less than the conventional wake with ten (five pairs) vortices. Turbulence and vortex injection both provide alleviation but for different reasons. Turbulence increases the rate of diffusion of vorticity thereby reducing wake velocities, whereas vortex injection induces convective redistribution of wake vorticity for reduced rolling moments.

CONCLUDING REMARKS

The results of the tests in the wind tunnel and water tow tank confirmed that alleviation of wake rolling moments can be achieved with a variety of fin configurations. Furthermore, it appears that fin configurations can be designed or optimized to minimize penalties in lift and drag and possibly to render them negligible. However, the large number of possible variations in fin design suggests that tests to follow should also attempt to accommodate the practical design constraints of the flight vehicle such as locations of the wing spars, fuel tanks, engines, and so on. These tests should also consider the use of blown flaps on the fins, the placement of three or more fins on each wing, and the use of other vortex generating devices in order to explore any special virtues of these configurations.

A review of the guidelines for fin design indicate that the original recommendations made in reference 16 are generally valid. That is, a large positive fin angle of attack (just below stall) is the most effective so that the fin size can be minimized. Also the fin or vortex generating device should be located on the B747 wing at about the center of the semispan. The optimum location was found to be more sensitive for the smaller fin sizes. Also, it was found that two fins near the optimum spanwise location provide more alleviation than one fin per side. Fins with Clark-Y or GA(W)-2 sections and with circular-arc planforms were particularly good because they brought about substantial wake alleviation with negligible penalties in lift and drag.

REFERENCES

1. Proceedings of NASA Symposium on Wake Vortex Minimization. NASA SP-409, 1976.

2. Croom, D. R.: Low-Speed Wind-Tunnel Investigation of Various Segments of Flight Spoilers as Trailing-Vortex-Alleviation Devices on a Transport Aircraft Model. NASA TN D-8162, 1976.

3. Croom, D. R.: Evaluation of Flight Spoilers for Vortex Alleviation. AIAA J. Aircraft, vol. 14, no. 8, 1977, pp. 823-825.

4. Corsiglia, V. R.; and Rossow, V. J.: Wind-Tunnel Investigation of the Effect of Porous Spoilers on the Wake of a Subsonic Transport Model. NASA TM X-73,091, 1976,

5. Patterson, J. C., Jr.; and Jordan, F. L., Jr.: Thrust Augmented Vortex Attenuation. Proceedings of NASA Symposium on Wake Vortex Minimization. NASA SP-409, 1976, pp. 258-274.

6. Rossow, V. J.: Theoretical Study of Lift-Generated Vortex Wakes Designed to Avoid Roll-Up. AIAA J., vol. 13, no. 4, 1975, pp. 476-484.

7. Rossow, V. J.: Convective Merging of Vortex Cores in Lift-Generated Wakes. AIAA J. Aircraft, vol. 14, no. 3, 1977, pp. 283-290.

8. Brandt, S. A.; and Iversen, J. D.: Merging of Aircraft Trailing Vortices. AIAA J. Aircraft, vol. 14, no. 12, 1977, pp. 1212-1220.

9. Corsiglia, V. R.; Orloff, K. L.; and Iversen, J. D.: Laser-Velocimeter Surveys of Merging Vortices in a Wind Tunnel. AIAA Paper 78-107, Jan. 1978.

10. Raj, P.; and Iversen, J. D.: Computational Studies of Turbulent Merger of Co-Rotational Vortices. AIAA Paper 78-108, Jan. 1978.

11. Hackett, J. E.; and Evans, P. F.: Numerical Studies of Three-Dimensional Breakdown in Trailing Vortex Wakes. AIAA J. Aircraft, vol. 14, no. 11, 1977, pp. 1093-1101.

12. Corsiglia, V. R.; Rossow, V. J.; and Ciffone, D. L.: Experimental Study of the Effect of Span Loading on Aircraft Wakes. AIAA J. Aircraft, vol. 13, no. 12, 1976, pp. 968-973.

13. Ciffone, D. L.: Vortex-Interactions in Multiple Vortex Wakes Behind Aircraft. AIAA J. Aircraft, vol. 14, no. 5, 1977, pp. 440-446.

14. Ciffone, D. L.; and Pedley, B.: Measured Wake Vortex Characteristics in Ground Effect. AIAA Paper 78-109, Jan. 1978.

15. Bilanin, A. J.; Teske, M. E.; and Hirsch, J. E.: The Role of Atmospheric Shear, Turbulence and a Ground Plane on the Dissipation of Aircraft Vortex Wakes. AIAA Paper 78-110, Jan. 1978.

16. Rossow, V. J.: Effect of Wing Fins on Lift-Generated Wakes. AIAA J. Aircraft, vol. 15, no. 3, 1978, pp. 160-167.

17. Dunham, R. E., Jr.: Exploratory Concepts Found to be Unsuccessful for Aircraft Wake Vortex Minimization. Proceedings of NASA Symposium on Wake Vortex Minimization. NASA SP-409, 1976, pp. 218-257.

18. Smith, A. M. O.: High-Lift Aerodynamics. AIAA J. Aircraft, vol. 12, no. 6, 1975, pp. 501-530.

19. Zimmerman, C. H.: Characteristics of Clark Y Airfoils of Small Aspect Ratios. NACA TR 431, 1932.

20. Liebeck, R. H.: A Class of Airfoils Designed for High Lift in Incompressible Flow. AIAA J. Aircraft, vol. 10, no. 10, Oct. 1973, pp. 610-617.

21. McGhee, R. J.; Beasley, W. D.; and Somers, D. M.: Low-Speed Aerodynamic Characteristics of a 13-Percent-Thick Airfoil Section Designed for General Aviation Applications. NASA TM X-72,697, 1977.

22. Polhamus, E. C.: A Concept of the Vortex Lift of Sharp-Edge Delta Wings Based on a Leading-Edge-Suction Analogy. NASA TN D-3767, 1966.

23. Lamar, J. E.: Prediction of Vortex Flow Characteristics of Wings at Subsonic and Supersonic Speeds. J. Aircraft, vol. 13, no. 7, 1976, pp. 490-494.

24. Kuhlman, J.: Load Distributions on Slender Delta Wings Having Vortex Flow. AIAA J. Aircraft, vol. 14, no. 7, 1977, pp. 699-702.

25. Wenzinger, C. J.; and Shortal, J. A.: The Aerodynamic Characteristics of a Slotted Clark Y Wing as Affected by the Auxiliary Airfoil Position. NACA TR 400, 1931.

26. Olson, L. E.: Optimization of Multielement Airfoils for Maximum Lift. NASA CP-2045, 1978.

27. Wei, M. H. Y.; and Corsiglia, V. R.: An Analysis of Coanda Jet Flows. NASA SP-228, 1969, pp. 197-214.

28. Levinsky, E. S.; and Yeh, T. T.: Analytical and Experimental Investigation of Circulation Control by Means of a Turbulent Coanda Jet. NASA CR-2114, 1972.

29. Hackett, J. E.; Boles, R. A.; and Lilley, D. E.: Ground Simulation and Tunnel Blockage for a Jet-Flapped, Basic STOL Model Tested to Very High Lift Coefficients. NASA CR-137,857, 1976.

30. Morehouse, G. G.; Eckert, W. T.; and Boles, R. A.: Aerodynamic Characteristics of a Small-Scale Straight and Swept-Back Wing with Knee-Blown Jet Flaps. NASA TM-78,427, 1977.

31. Rossow, V. J.; Corsiglia, V. R.; and Phillippe, J. J.: Measurements of the Vortex Wakes of a Subsonic- and a Supersonic-Transport Model in the 40- by 80-Foot Wind Tunnel. NASA TM X-62,391, 1974.

32. Hough, G.: Remarks on Vortex-Lattice Methods. AIAA J. Aircraft, vol. 10, no. 5, 1973, pp. 314-317.

TABLE I.- MODEL DIMENSIONS AND WIND-TUNNEL CONDITIONS

(Scale = 0.03)

Model dimensions	
Following model	
Span, cm (in.)	33.3 (13.1)
Chord, cm (in.)	6.1 (2.4)
Aspect ratio	5.5
Wing planform	Rectangular
Wing section	NACA 0012
Fuselage diameter, cm (in.)	5.1 (2.0)
Balance full-scale range, N-m (in.-lb)	3.4 (30)
α_f, deg	0
Generator model	
Wing	
Span, cm (in.)	179 (70.5)
Root incidence, deg	+2
Tip incidence, deg	-2
Area, m^2 (ft^2)	0.459 (4.94)
Average chord, cm (in.)	25.6 (10.1)
Aspect ratio	7
Horizontal stabilizer, deg	0
Flaps	$(30°/30°)^3$
Landing gear deployed	

Test parameters	Wind tunnel	Water tow tank
U_∞	40 m/s (131 ft/s)	3.8 m/s (12.5 ft/s)
Re	660,000	814,000
x_f/b_g	14	46
q_∞	958 N/m^2 (20 lb/sq ft)	7280 N/m^2 (152 lb/sq ft)
α_g	4° (C_{L_g} = 1.24)	5° (C_{L_g} = 1.2)

TABLE II.- DATA FROM WIND-TUNNEL TESTS; $\alpha_g = 4°$, $x_f/b_g = 14$

Configuration	Fins/wing	Fin planform (cross section)	$\frac{c_{fin}}{b_g}$	$\frac{h_{fin}}{b_g}$	α_{fin}	Midchord location of fin		C_{L_g}	C_{D_g}	C_{l_f}	
						$\frac{x_{fin}}{b_g/2}$	$\frac{y_{fin}}{b_g/2}$			Port	Starboard
First tunnel entry											
1	0	---	---	---	---	---	---	1.24	0.25	-0.104	0.117
2	1	Rectangular (flat plate)	0.0426	0.0851	-12°	1.287	0.702	1.30	.29	-.101	.127
3	1	↓	↓	↓	12°	1.282	.702	1.25	.30	-.076	.072
4	1	↓	↓	↓	18°	1.279	.702	1.17	.32	-.067	.058
5	1	↓	↓	↓	12°	1.282	.993	1.34	.30	-.110	.111
6	1	↓	0.0851	0.0567	12°	1.282	.702	1.08	.30	-.091	.074
7	1	↓	0.0851	0.0567	18°	1.279	.702	1.15	.32	-.074	.069
8	1	↓	0.0851	0.0567	18°	1.094	.485	1.19	.31	---	.033
Second tunnel entry											
1	0	---	---	---	---	---	---	1.24	0.25	-0.104	-0.117
2	1	Rectangular (flat plate)	0.0851	.0071	18°	1.094	0.485	1.27	.27	-.075	.089
3	↓	↓	↓	.0142	12°	1.096	↓	1.27	.28	---	.072
4	↓	↓	↓	.0142	18°	1.094	↓	1.24	.28	-.048	.052
5	↓	↓	↓	.0142	24°	1.091	↓	1.18	.29	-.033	.047
6	↓	↓	↓	.0284	18°	1.094	↓	1.18	.29	-.033	.042
7	↓	↓	↓	.0426	18°	1.094	↓	1.18	.31	-.034	.040
8	↓	↓	↓	.0567	18°	1.094	↓	1.18	.32	-.029	.031
9	↓	↓	.1277	.0142	12°	1.096	↓	1.28	.27	-.064	.064
10	↓	↓	↓	↓	18°	1.094	↓	1.27	.29	-.033	.048
11	↓	↓	↓	↓	24°	1.091	↓	1.27	.30	-.035	.053
12	↓	↓	↓	↓	18°	1.052	.403	1.28	.29	---	.089
13	↓	↓	↓	↓	↓	1.150	.544	1.27	.29	-.047	.056
14	↓	↓	↓	.0284	↓	1.094	.485	1.22	.31	-.041	.042
15	↓	↓	↓	.0426	↓	1.094	.485	1.18	.33	-.038	.040
16	↓	↓	↓	.0567	↓	1.094	.485	1.18	.35	-.035	.045

TABLE II.- Continued.

Configuration	Fins/wing	Fin planform (cross section)	$\frac{c_{fin}}{b_g}$	$\frac{h_{fin}}{b_g}$	α_{fin}	Midchord location of fin		C_{L_g}	C_{D_g}	C_{l_f}	
						$\frac{x_{fin}}{b_g/2}$	$\frac{y_{fin}}{b_g/2}$			Port	Starboard
Third tunnel entry											
1	0	---	---	---	---	---	---	1.25	0.25	-0.104	0.121
2	1	Rectangular	0.0851	0.0567	18°	1.094	0.485	1.09	.28	-.035	.027
3	1	Triangular	.0737	.0426	18°	1.112	↓	1.25	.27	-.072	.075
4	1	(flat plate)	.0737	.0426	24°	1.112	↓	1.23	.27	-.056	.061
5	1	↓	.0737	.0426	30°	1.112	↓	1.20	.27	-.058	.059
6	2	↓	.0737	.0426	24°	1.050, 1.098	.442, .516	1.18	.28	-.029	.037
7	2	↓	.0491	.0284	↓	1.059, 1.107	.442, .516	1.22	.28	-.076	---
8	2	↓	.0615	.0355	↓	1.054, 1.102	.442, .516	1.21	.28	-.048	.043
9	2	↓	.0615	.0355	↓	1.054, 1.116	.442, .485	1.20	.28	-.051	.050
10	2	↓	.0615	.0355	↓	1.054, 1.132	.442, .544	1.20	.28	-.051	.055
11	1	Circular arc (Clark Y)	.0709	.0355	18°	1.094	.485	1.25	.28	-.044	.053
12	1	(Clark Y)	↓	↓	30°	1.088	↓	1.22	.28	-.038	.046
13	1	(Clark Y)	↓	↓	36°	1.082	↓	1.16	.28	-.037	.040
14	1	(GA(W)2)	↓	↓	18°	1.094	↓	1.26	.27	-.039	.063
15	1	(GA(W)2)	↓	↓	30°	1.088	↓	1.18	.27	-.039	.043
16	1	(GA(W)2)	↓	↓	36°	1.082	↓	1.18	.27	-.037	.045
17	1	(Clark Y)	.0567	.0284	30°	1.088	↓	1.24	.28	-.042	.055
18	1	(Clark Y)	.0425	.0213	30°	1.088	↓	1.25	.27	-.056	.076
19	1	↓	↓	↓	24°	1.091	↓	1.25	.27	-.055	.081
20	1	↓	↓	↓	30°	1.065	.442	1.25	.27	-.057	.064
21	1	↓	↓	↓	30°	1.045	.403	1.25	.27	-.083	.101

TABLE II.- Concluded.

Configuration	Fins/wing	Fin planform (cross section)	$\frac{c_{fin}}{b_g}$	$\frac{h_{fin}}{b_g}$	α_{fin}	Midchord location of fin		C_{L_g}	C_{D_g}	C_{l_f}	
						$\frac{x_{fin}}{b_g/2}$	$\frac{y_{fin}}{b_g/2}$			Port	Starboard
Third tunnel entry (Continued)											
22	1	Circular arc	0.0425	0.0213	30°	1.113	0.516	1.25	0.27	-0.080	0.083
23	1	(Clark Y)	.0284	.0142	30°	1.088	.485	1.25	.26	-.088	.096
24	1	(Clark Y)	.0284	.0142	24°	1.091	.485	1.25	.26	-.092	.102
		(Clark Y)									
25	2	(Clark Y)	.0425	.0213	30°	1.045	.403	1.20	.28	-.040	.042
		(GA(W)2)				1.088	.485				
26	2	(Clark Y)	.0425	.0213	30°	1.065	.442	1.18	.28	-.041	.037
		(GA(W)2)				1.113	.516				
27	2	(Clark Y)	.0284	.142		1.065	.442	1.18	.27	-.045	.073
		(GA(W)2)				1.113	.516				
28	2	(Clark Y)				1.045	.403	1.28	.28	-.086	.087
		(GA(W)2)				1.113	.516				
29	2	(Clark Y)				1.065	.442	1.25	.28	-.045	.067
		(GA(W)2)				1.143	.544				
30	1	Rectangular (1 element)	.0142	.0142	24°	1.091	.482	1.28	.27		.114
31	1	(2 element)	.028	.0142	24°	1.091	.482	1.29	.28	---	.092
32	1	(2 element)	.028	.0284	18°	1.094	.482	1.28	.27	-.092	.106
33	1	(2 element)	.028	.0284	24°	1.091	.482	1.28		-.074	.111
34	1	(3 element)	.042	.0142	18°	1.072	.440	1.25		-.061	.078
35	1	(3 element)	.042	.0142	12°	1.083	.440			-.063	.078
36	1	(3 element)	.042	.0284	12°	1.083	.440			-.092	.106
37	2	Rectangular (flat plate)	.0284	.0142	24°	1.068	.442		.28	-.059	.064
					24°	1.165	.530				
38	1	Blown flap			12°	1.090	.461		.27	-.083	.105
39	1	Blown flap			24°	1.090	.461	1.24	.28	-.056	.075

TABLE III.- DATA FROM TESTS IN WATER TOW TANK — CIRCULAR ARC FINS; $\alpha_g = 5°$, $x_f/b_g \approx 46$.

Configuration	Fins/wing	Airfoil section	$\frac{c_{fin}}{b_g}$	$\frac{h_{fin}}{b_g}$	α_{fin}	Midchord location of fin		C_{L_g}	C_{D_g}	C_{M_g}	C_{l_f}	
						$\frac{x_{fin}}{b_g/2}$	$\frac{y_{fin}}{b_g/2}$				Port	Starboard
1	0	---	---	---	---	---	---	1.200	0.200	-0.227	---	0.115
2	1	Clark Y	0.0425	0.0213	18°	1.068	0.442	1.209	.190	-.173	---	.0929
3	1	↓	↓	↓	24°	1.068	.442	1.167	.204	-.149	-0.0587	.0587
4	1	↓	↓	↓	30°	1.068	.442	1.186	.196	-.168	---	.0709
5	1	↓	↓	↓	24°	1.048	.403	1.217	.189	-.208	-.0978	.1124
6	1	↓	↓	↓	↓	1.091	.485	1.166	.208	-.165	-.0636	.0743
7	1	↓	↓	↓	↓	1.116	.516	1.201	.192	-.191	-.0782	.0772
8	1	↓	↓	↓	↓	1.146	.544	1.200	.192	-.199	---	.0836
9	1	↓	.0284	.0142	↓	1.068	.442	1.199	.181	-.199	---	.0987
10	1	↓	.0213	.0106	↓	1.068	.442	1.219	.176	-.216	---	.1026
11	1	↓	.0709	.0355	↓	1.068	.442	1.157	.220	-.107	-.0635	.0655
12	1	↓	.0709	.0355	↓	1.091	.485	1.161	.218	-.126	-.0391	.0460
13	2	Clark Y	.0425	.0213	↓	1.068	.442	1.164	.215	-.123	-.0550	.0538
		GA(W)2	.0425	.0213	↓	1.116	.516					
14	2	Clark Y	.0425	.0213	↓	1.091	.485	1.165	.215	-.128	-.0474	.0470
		GA(W)2	.0425	.0213	↓	1.146	.544					
15	2	Clark Y	.0284	.0142	↓	1.068	.442	1.170	.191	-.172	-.0640	.0782
		GA(W)2	.0284	.0142	↓	1.116	.516					
16	2	Clark Y	.0284	.0142	↓	1.091	.485	1.186	.195	-.179	-.0665	.0660
		GA(W)2	.0284	.0142	↓	1.146	.544					
17	2	Clark Y	.0213	.0106	↓	1.091	.485	1.199	.186	-.203	-.0733	.0890
		GA(W)2	.0213	.0106	↓	1.146	.544					

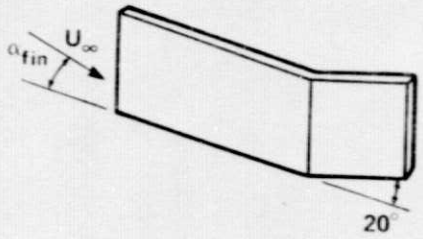

A. RECTANGULAR PLANFORM; BENT FLAT PLATE SECTIONS, $C_{L_{max}} \approx 1.$

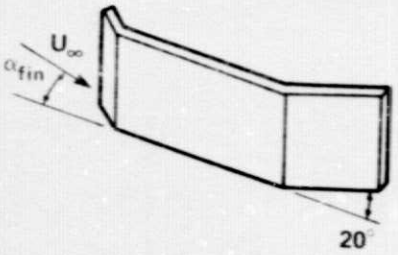

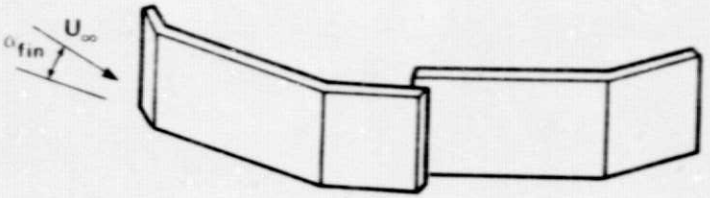

B. MULTI-ELEMENT OF RECTANGULAR PLANFORMS; BENT FLAT PLATE SECTIONS, $C_{L_{max}} \approx 2.$

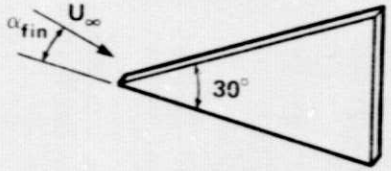

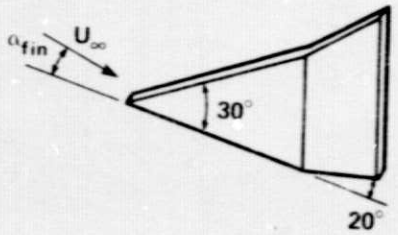

C. TRIANGULAR PLANFORMS, FLAT PLATE SECTIONS, $C_{L_{max}} \approx 1.2.$

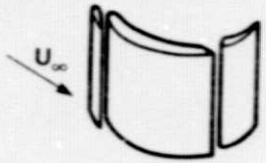

D. RECTANGULAR PLANFORMS; AIRFOIL SECTIONS, $C_{L_{max}} \approx 3.$

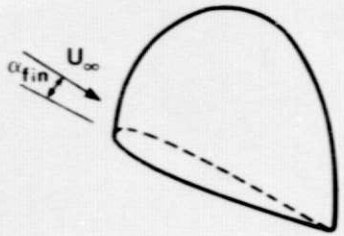

E. CIRCULAR ARC PLANFORM; CLARK Y OR GA(W)2 SECTION, $C_{L_{max}} \approx 2.$

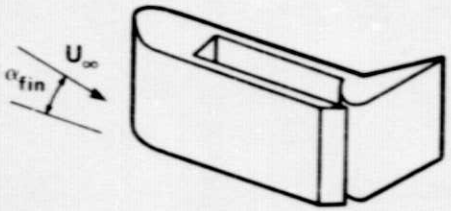

F. RECTANGULAR PLANFORM; SHAPED AIRFOIL WITH BLOWN FLAP, $C_{L_{max}} \approx 10.$

Figure 1.- Schematic diagrams of fin shapes used in tests.

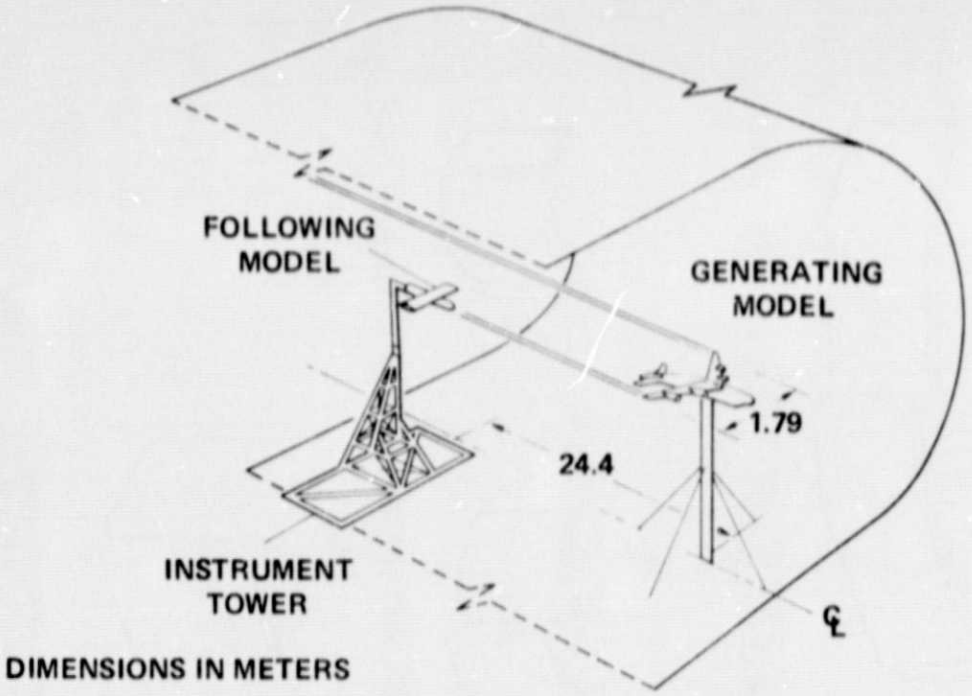

(a) Diagram of setup.

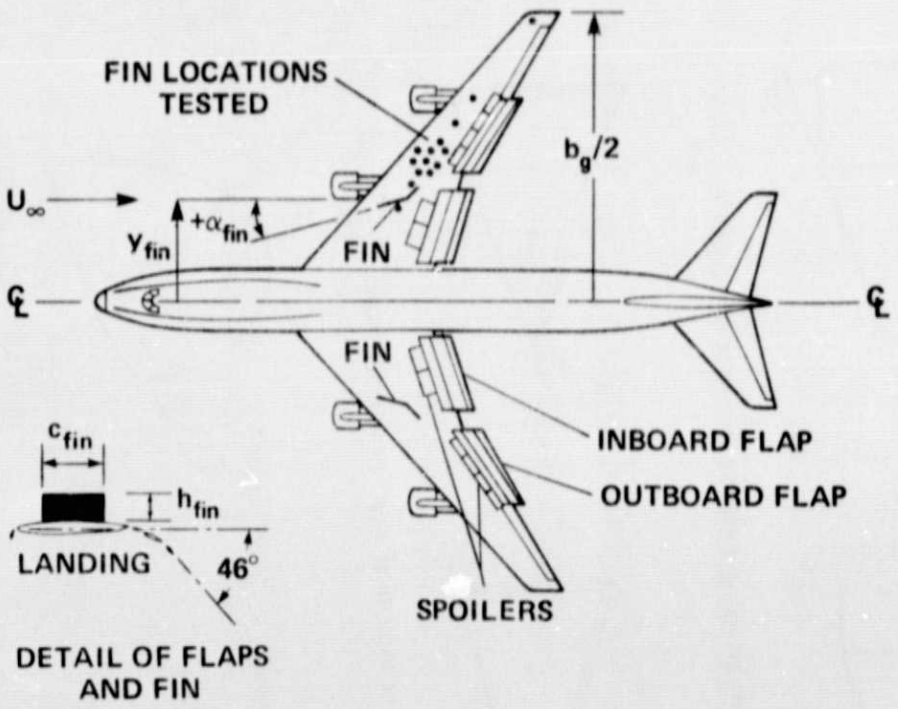

(b) Plan view of generator model; dots on starboard wing indicate test locations of center of fin chord.

Figure 2.- Experimental setup in the NASA-Ames Research Center 40- by 80-Foot Wind Tunnel.

(c) Closeup view of B747 model tunnel with two circular arc fins mounted on each wing.

Figure 2.- Continued.

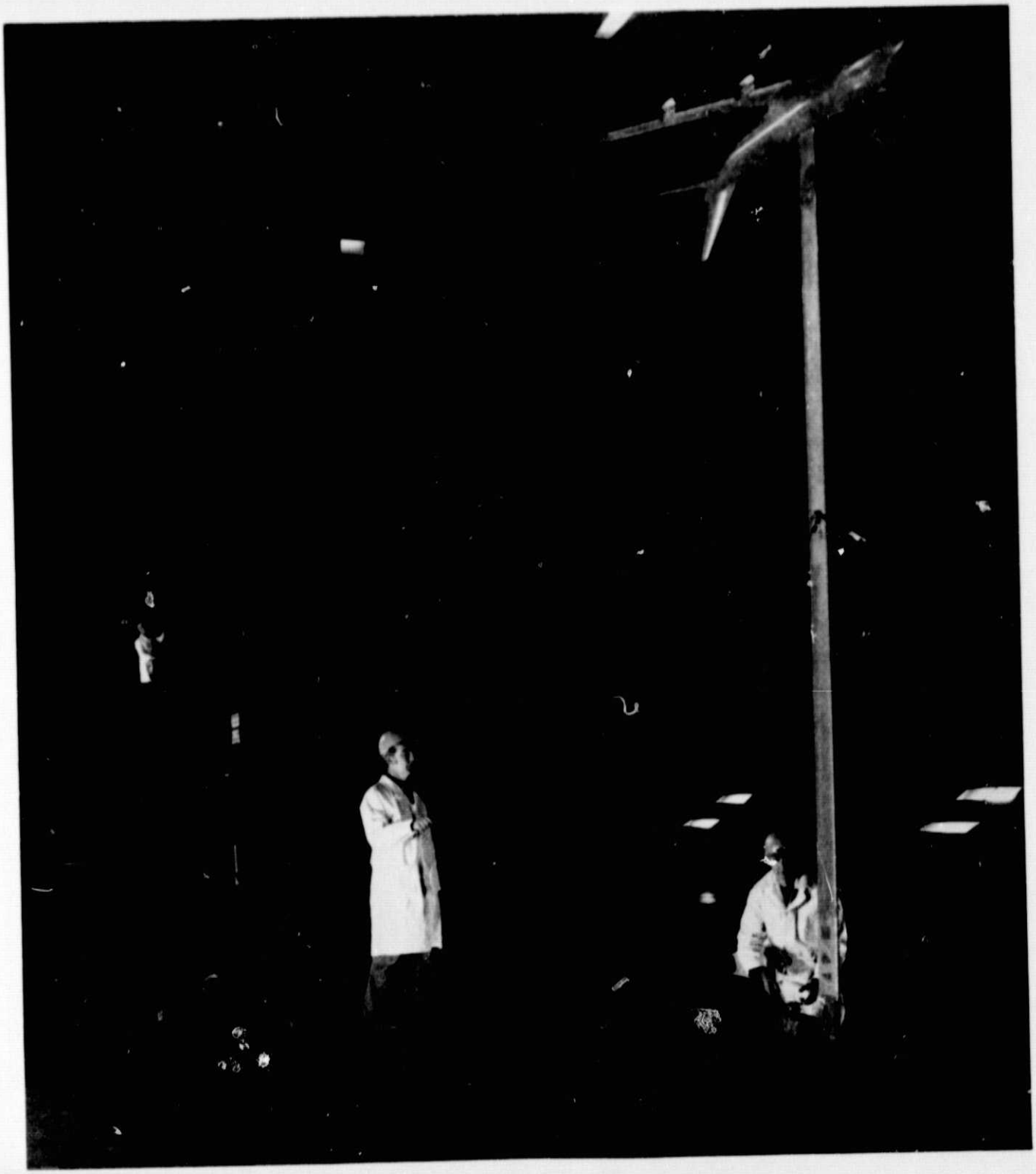

(d) Photograph of test setup.

Figure 2.- Concluded.

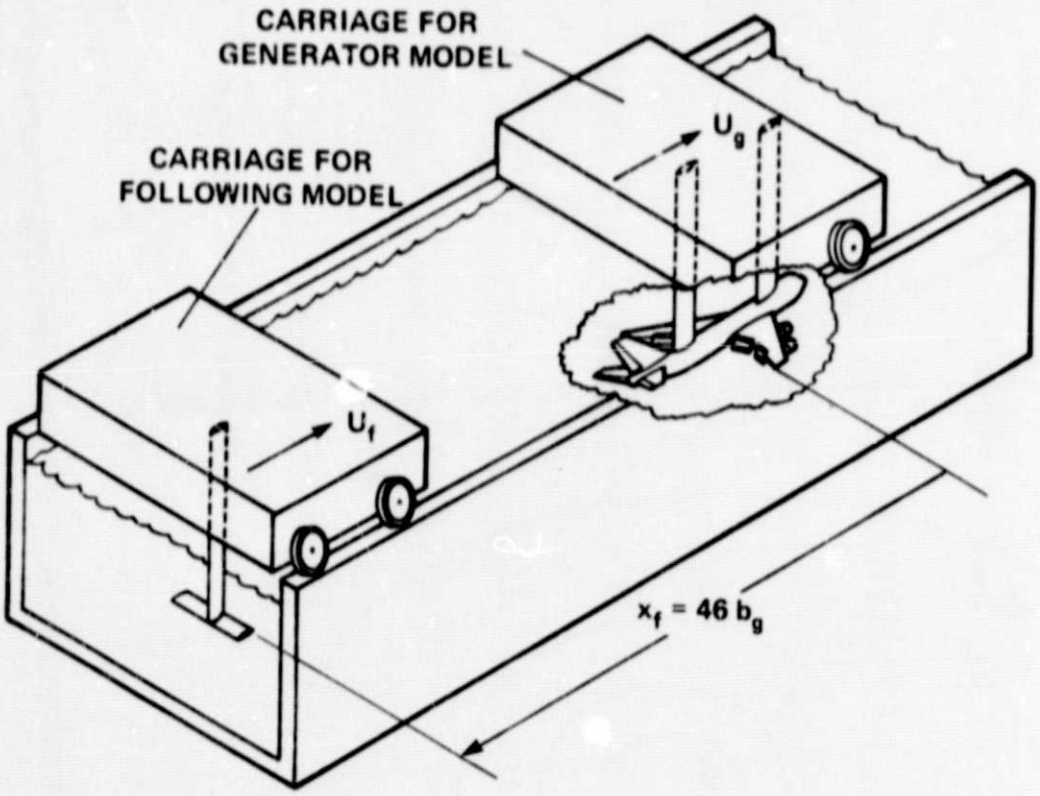

Figure 3.- Schematic diagram of water tow tank and carriage arrangement at Hydronautics, Inc.; $U_f = U_g = 3.8$ m/s (12.5 ft/s), tank length = 125 m (410 ft), width = 7.6 m (24 ft), depth = 3.8 m (12.5 ft).

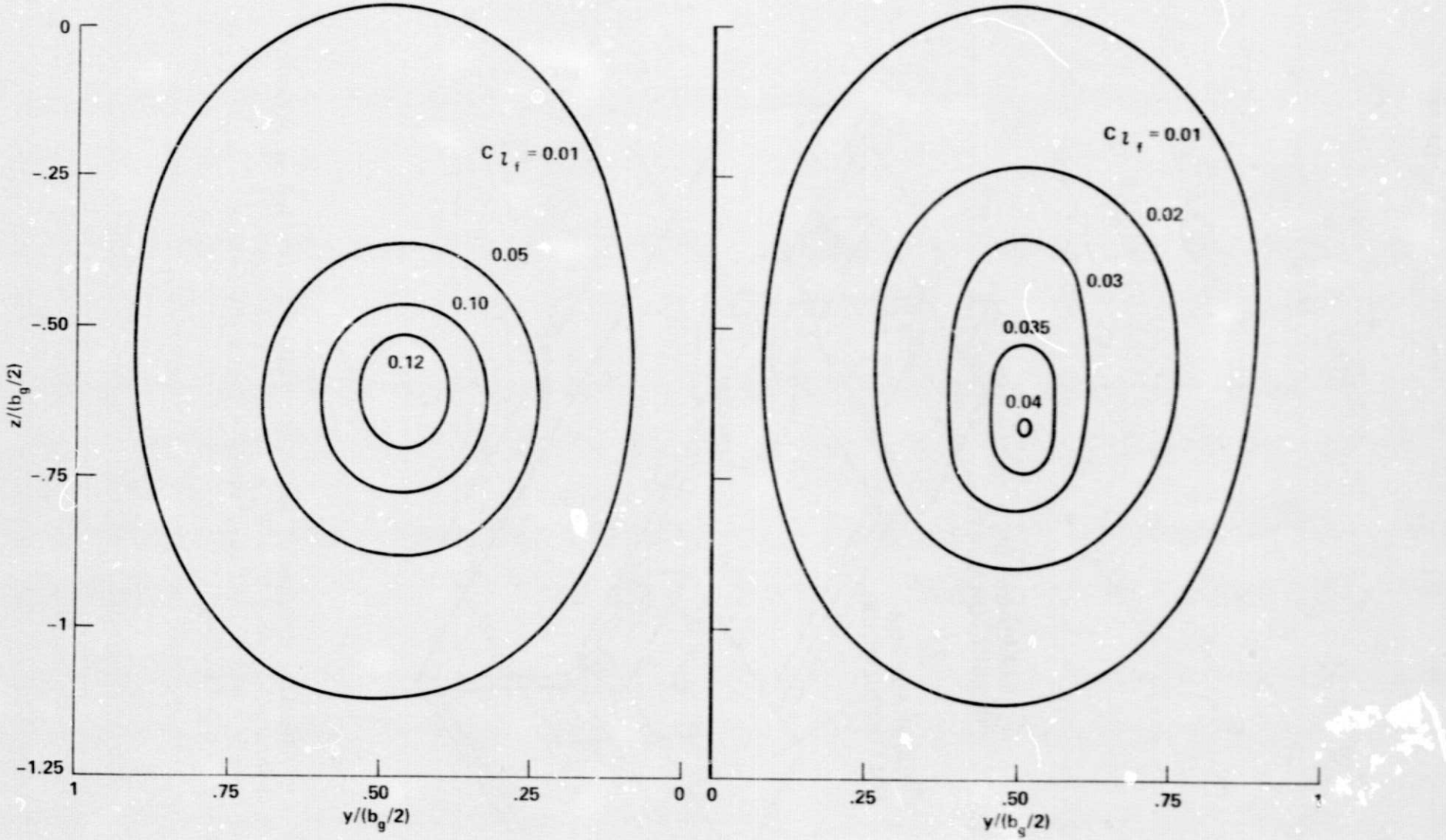

A. CONVENTIONAL LANDING CONFIGURATION.

B. LANDING CONFIGURATION WITH ONE RECTANGULAR FIN/SIDE; $h_{fin} = c_{fin} = 0.085\ b_g$, $\alpha_{fin} = 12°$, $y_{fin}/(b_g/2) = 0.50$.

Figure 4.- Contours of equal rolling moment as measured on following model in wake of model of B747 in 40- by 80-foot wind tunnel; $\alpha_g = 4°$, $x_f/b_g = 14$.

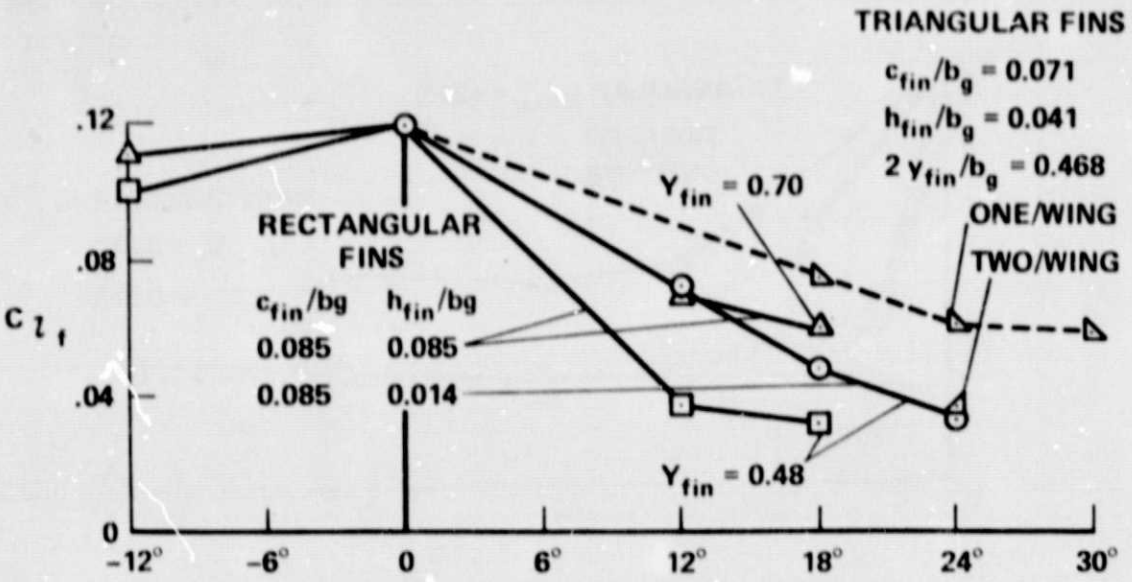

Figure 5.- Variation of rolling moment in starboard side of wake with angle of attack of rectangular and triangular fins; $\alpha_g = 4°$, $x_f/b_g = 14$.

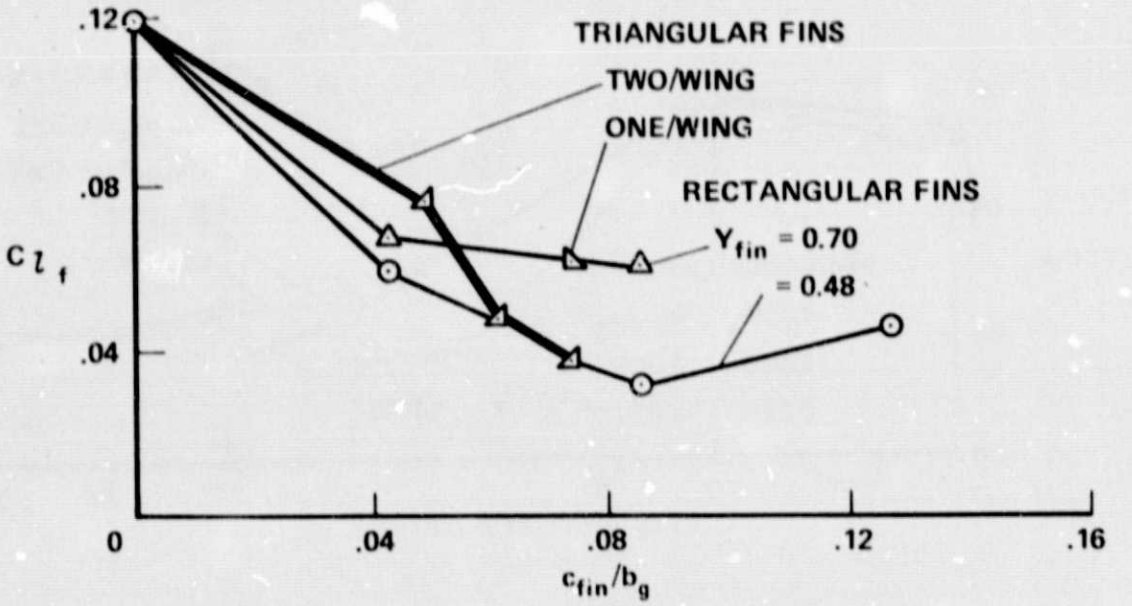

Figure 6.- Variation of rolling moment in starboard side of wake with chord of rectangular ($h_{fin}/b_g = 0.085$, $\alpha_{fin} = +18°$) and triangular ($\alpha_{fin} = 24°$) fins; $\alpha_g = 4°$ ($C_{L_g} \approx 1.2$), $x_f/b_g = 14$.

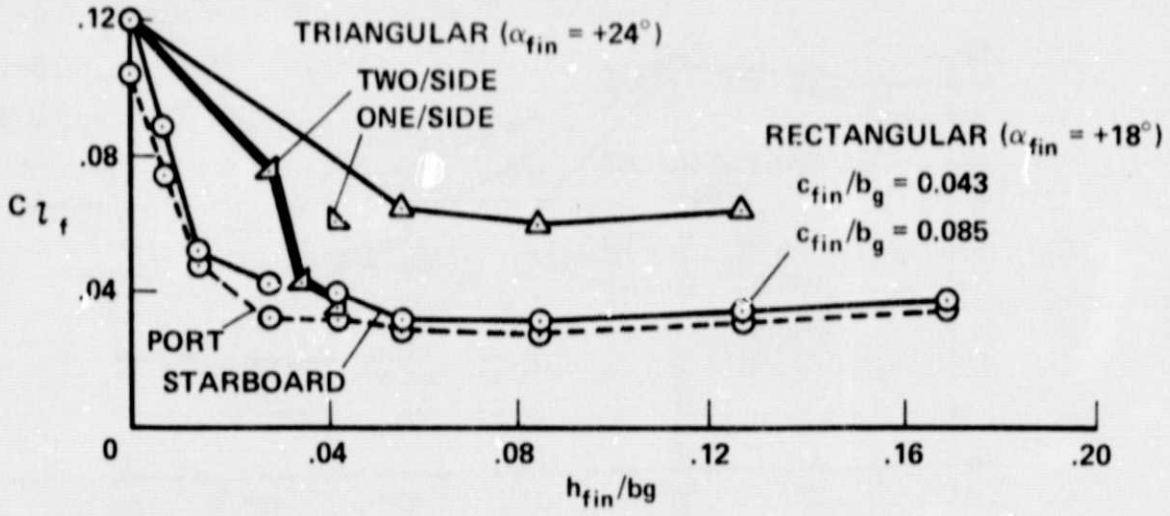

Figure 7.- Variation of wake rolling moment with fin height; $\alpha_g = 4°$, $x_f/b_g = 14$.

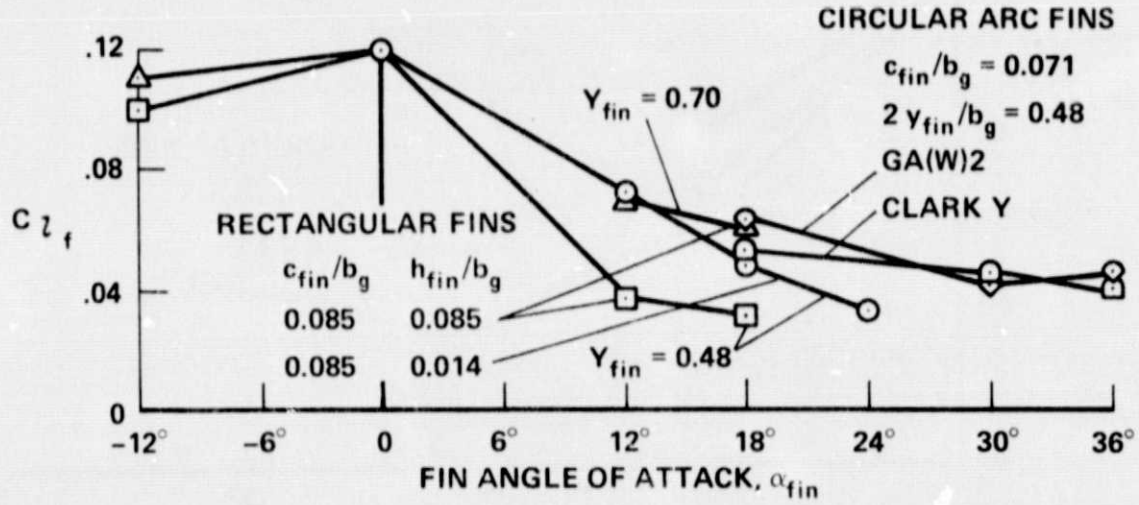

Figure 8.- Variation of rolling moment in starboard side of wake with angle of attack of rectangular and circular arc fins; $\alpha_g = 4°$, $x_f/b_g = 14$.

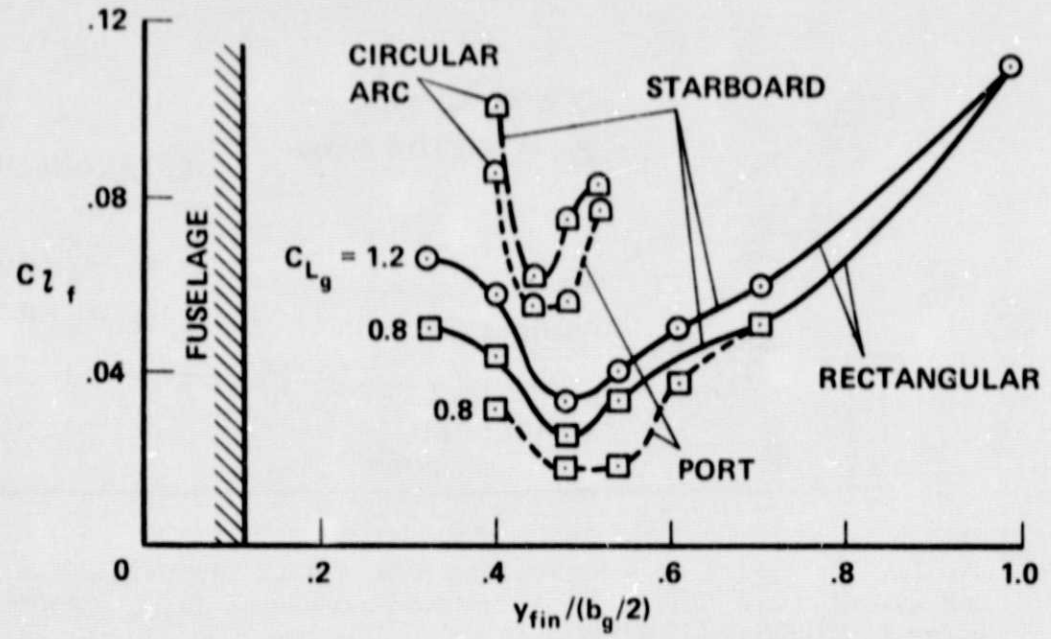

Figure 9.- Variation measured in wind tunnel of wake rolling moment with spanwise location of fin; rectangular fin, $c_{fin}/b_g = 0.085$, $h_{fin}/b_g = 0.085$, $\alpha_{fin} = +18°$; circular arc fin, $c_{fin}/b_g = 0.043$, $\alpha_{fin} = 30°$.

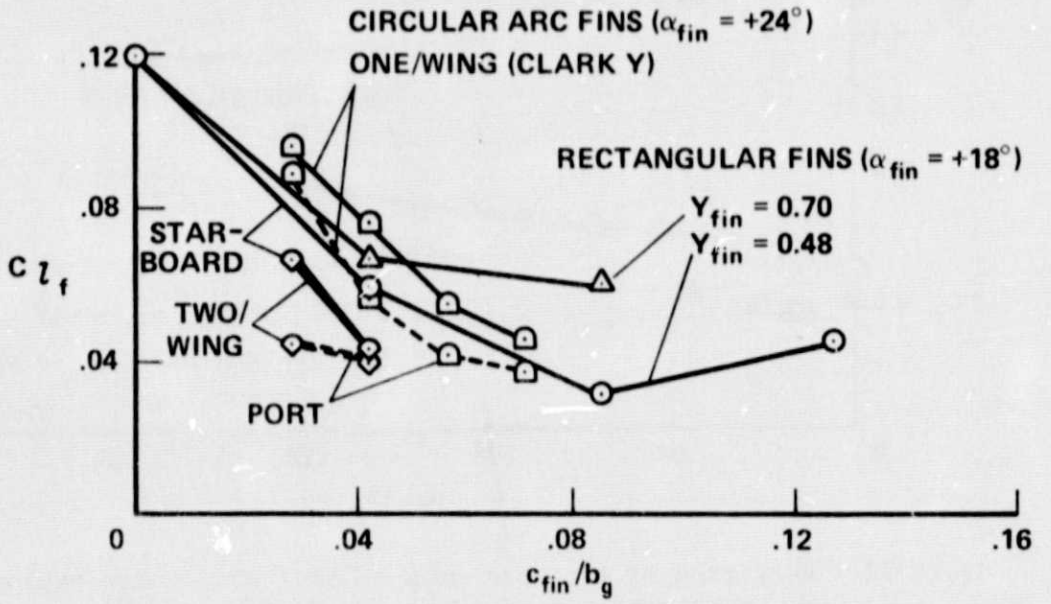

Figure 10.- Variation of wake rolling moment with chord of circular arc and rectangular ($h_{fin}/b_g = 0.085$) fins; $\alpha_g = 4°$ ($C_{L_g} \approx 1.2$), $x_f/b_g = 14$.

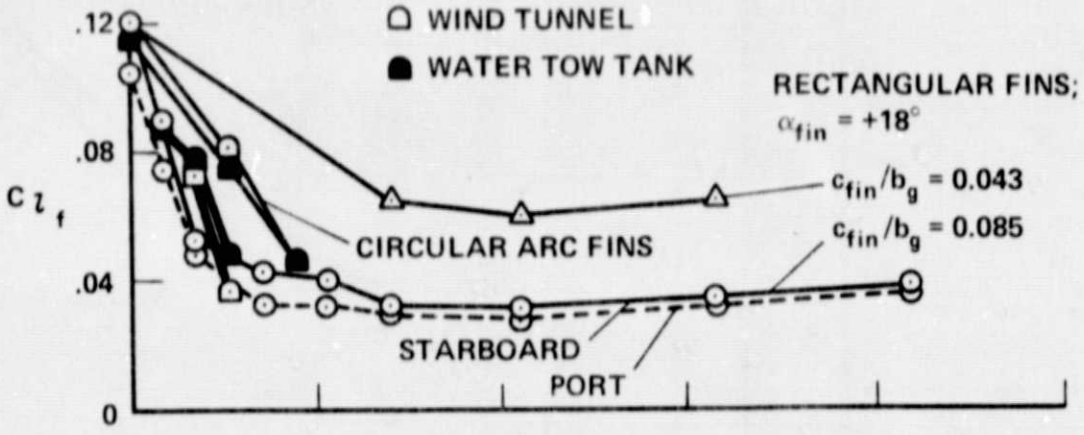

Figure 11.- Variation of wake rolling moment with fin height for rectangular and circular arc fins as measured in wind tunnel (α_{fin} = +30°) and water tow tank (α_{fin} = +24°).

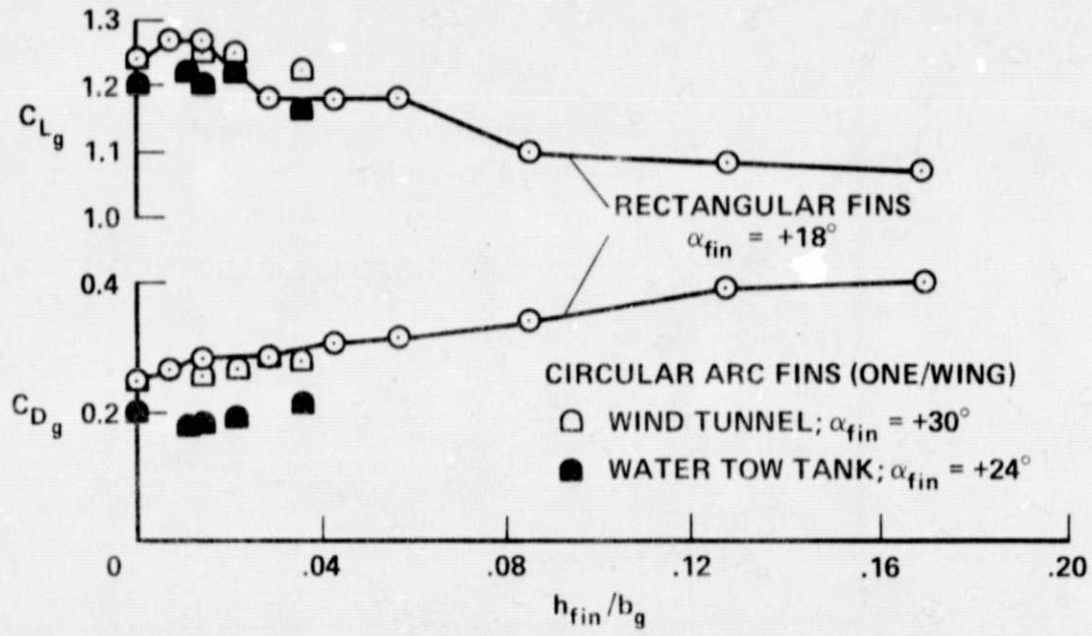

Figure 12.- Variation of lift and drag of B747 model when equipped with rectangular or circular arc fins; α_g = +4°.

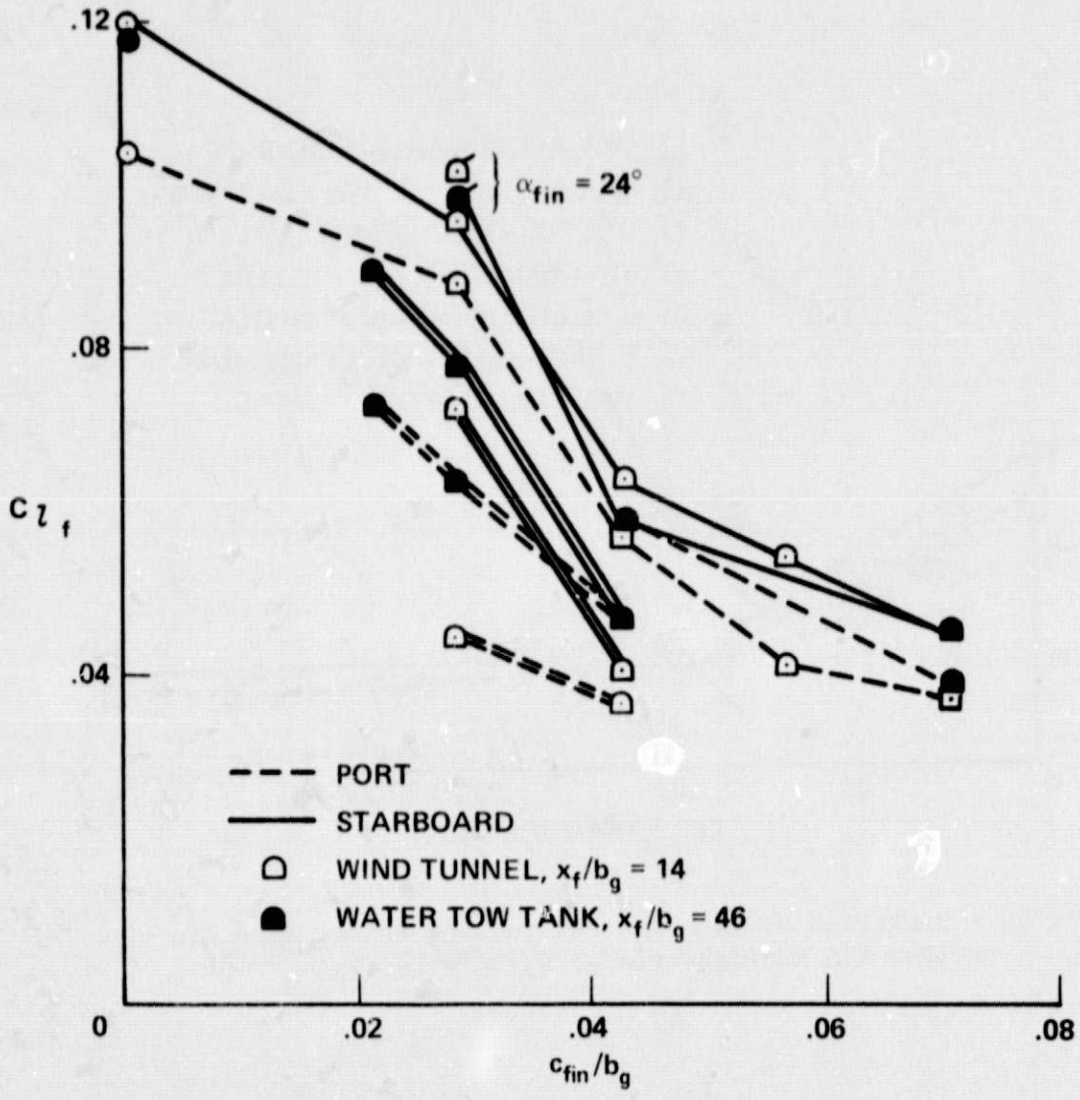

Figure 13.- Comparison of rolling moments measured in wakes modified by circular arc fins in wind tunnel with result from water tow tank.

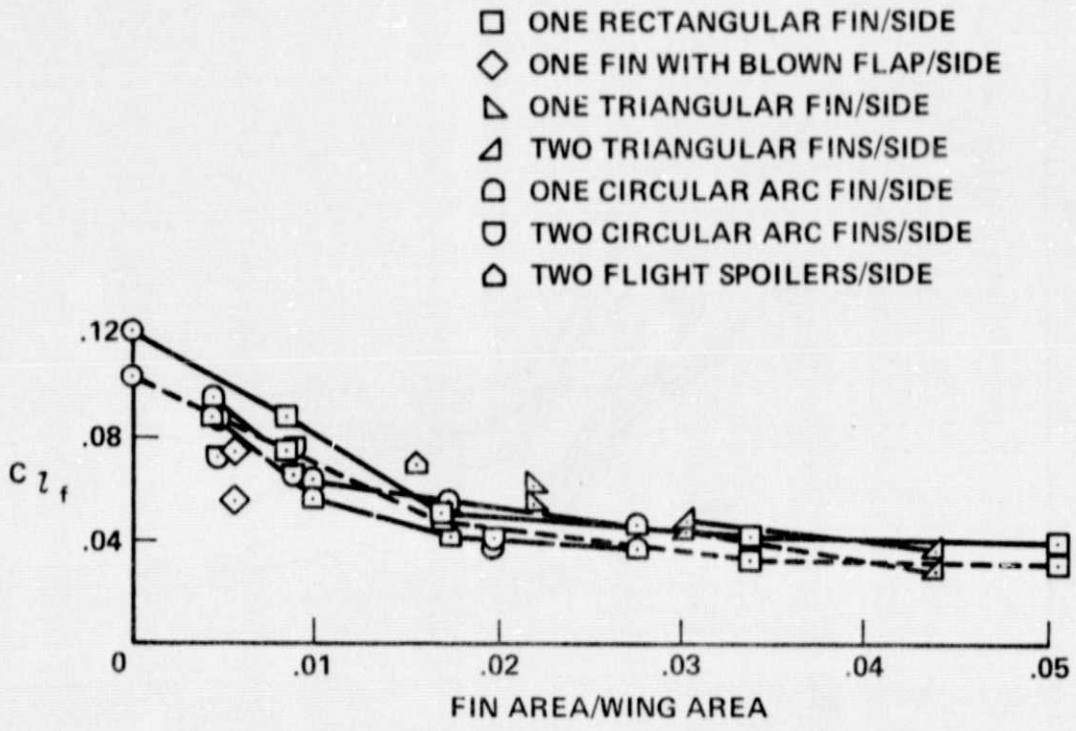

Figure 14.- Variation of wake-induced rolling moment with fin size for various fin configurations; $x_f/b_g = 14$, $b_f/b_g = 0.19$.

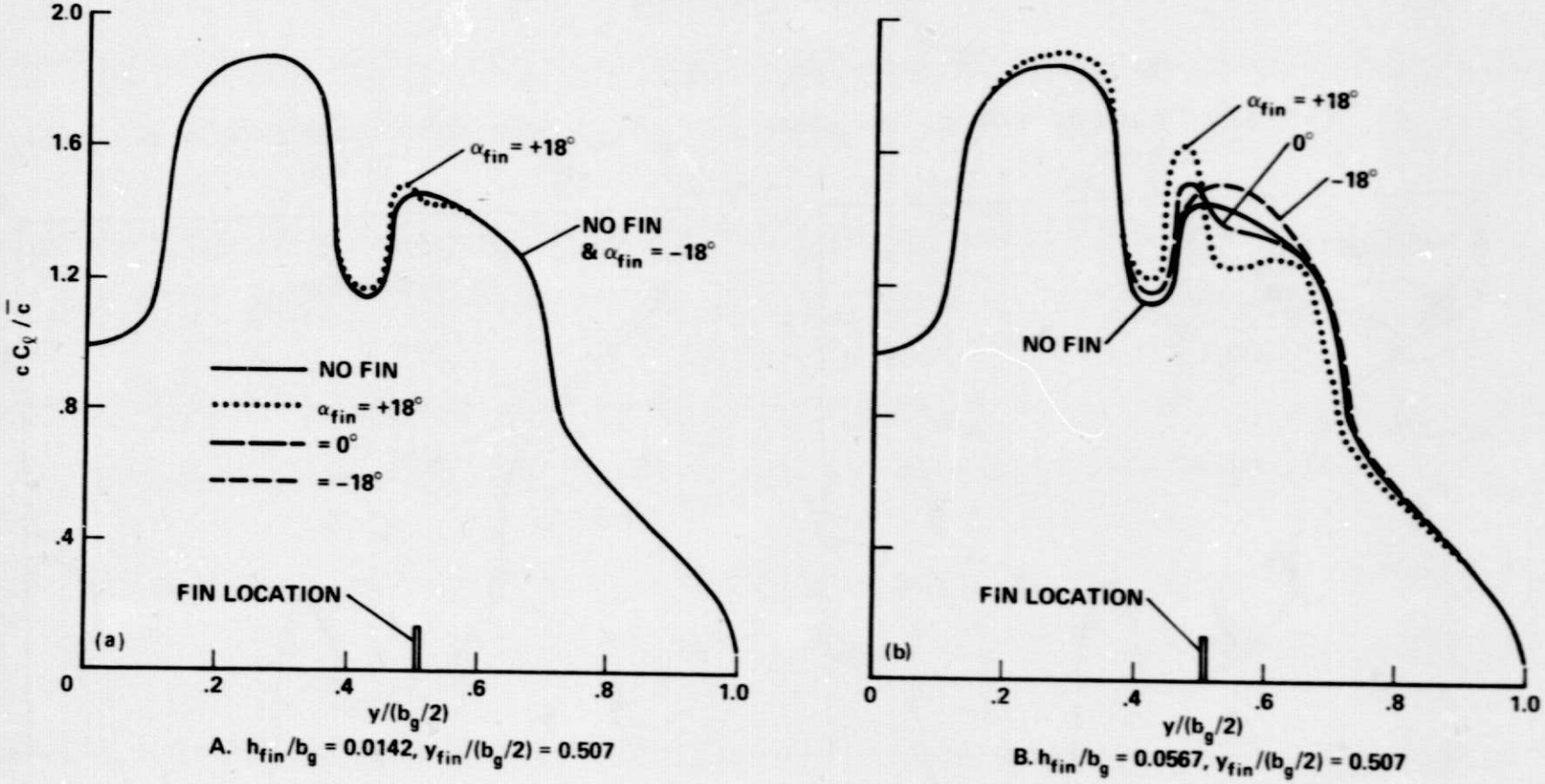

Figure 15.- Span loadings predicted by vortex-lattice theory for wing of Boeing 747 (30°/30°) model equipped with various fin sizes, locations and angles of attack; $\alpha_g = 4°$, $c_{fin}/b_g = 0.083$, $C_L \approx 1.18$, $C_{D_i} \approx 0.115$.

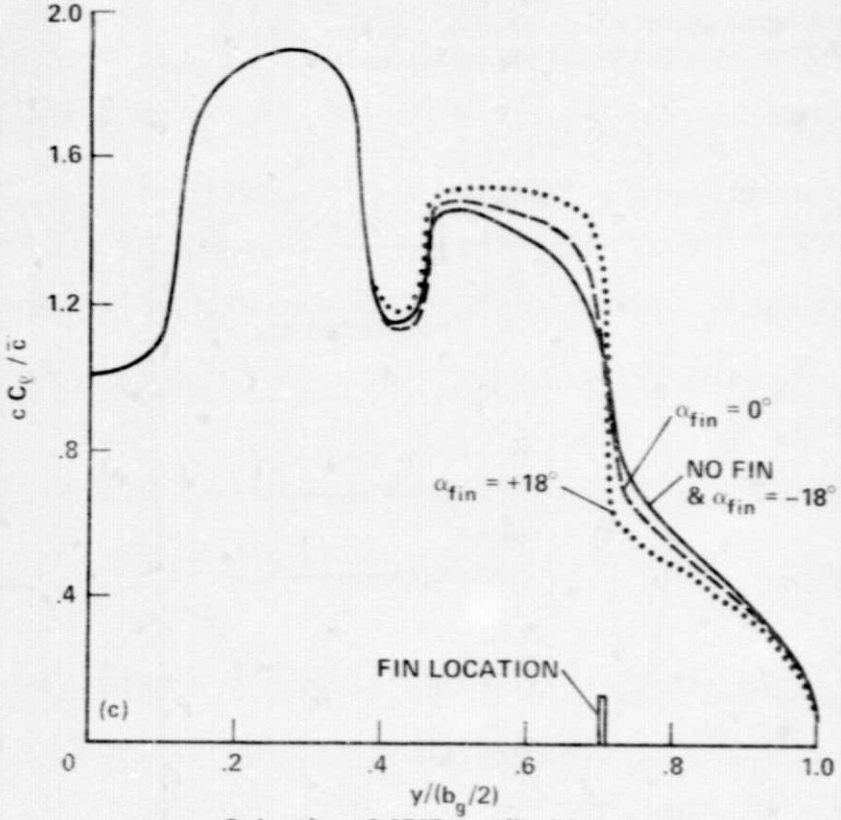

C. $h_{fin}/b_g = 0.0567$, $y_{fin}/(b_g/2) = 0.704$

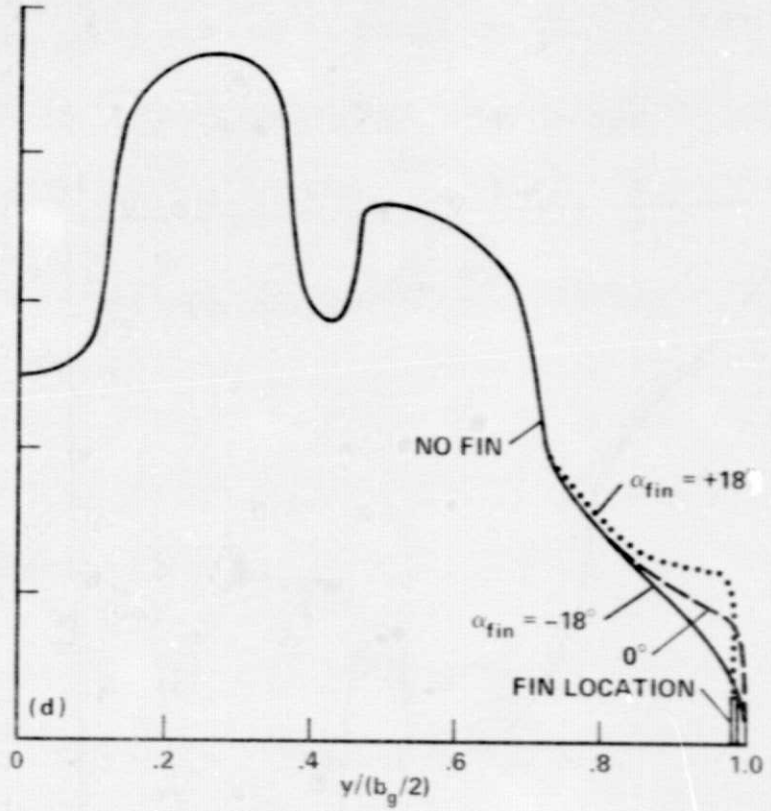

D. $h_{fin}/b_g = 0.0567$, $y_{fin}/(b_g/2) = 0.986$

Figure 15.- Concluded.

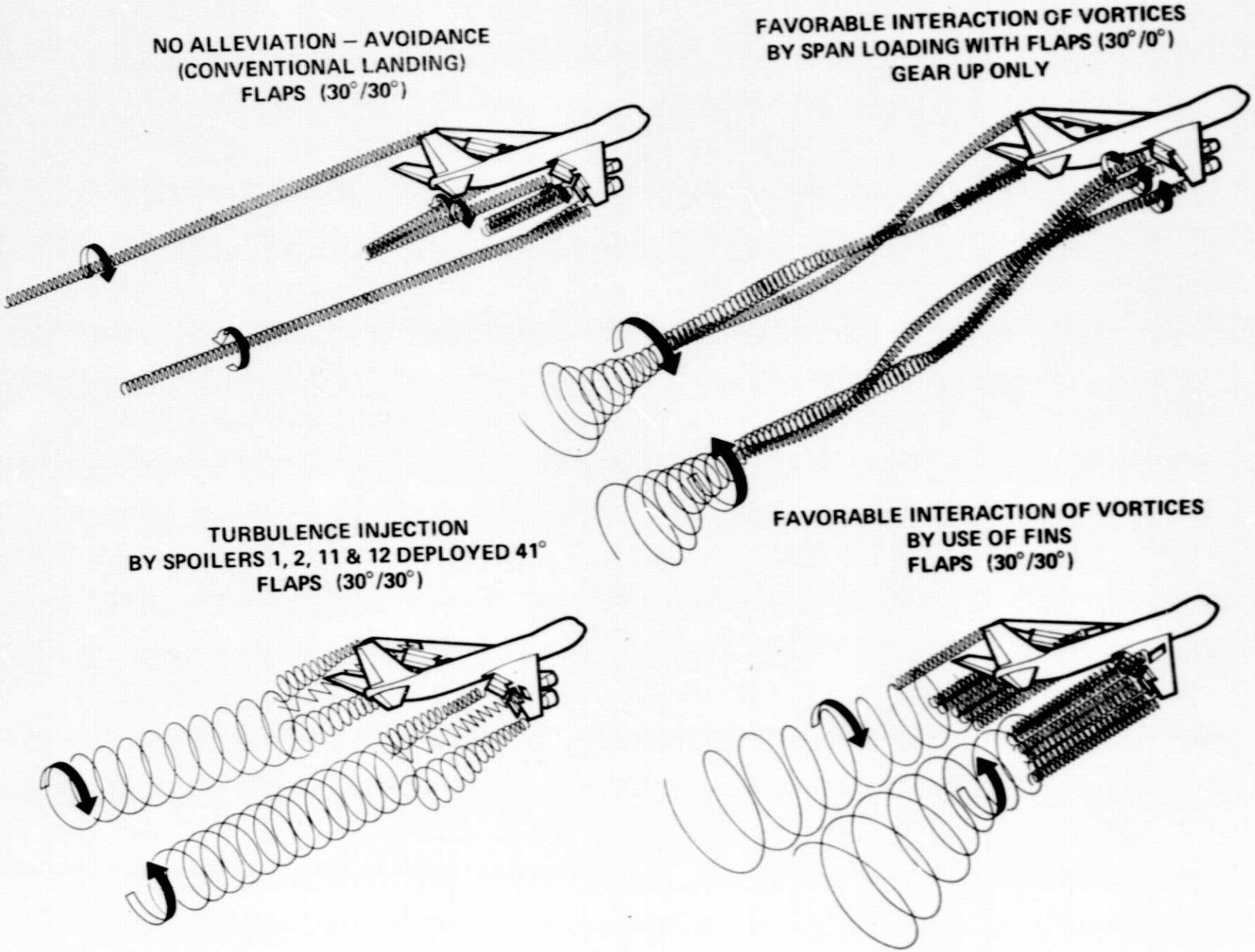

Figure 16.- Current methods for reducing wake hazard.